International Environmental Modelling and Software Society (iEMSs)
7th Intl. Congress on Env. Modelling and Software, San Diego, CA, USA,
Daniel P. Ames, Nigel W.T. Quinn and Andrea E. Rizzoli (Eds.)
http://www.iemss.org/society/index.php/iemss-2014-proceedings

Physically based landslide susceptibility models with different degree of complexity: calibration and verification

Giuseppe Formetta[a], Giovanna Capparelli[a], Riccardo Rigon[b] and Pasquale Versace[a]

[a]*University of Calabria, Civil and Environmetal Engineering Department (giuseppe.formetta@unical.it, giovanna.capparelli@unical.it, pasquale.versace@unical.it)*

[b]*University of Trento, Civil and Environmetal Engineering Department (riccardo.rigon@ing.unitn.it)*

Abstract: Rainfall induced shallow landslides cause significant damages involving loss of life and properties. Predict shallow landslides susceptible locations is a complex task that involves many disciplines: hydrology, geotechnical science, geomorphology, statistics. Usually to accomplish this task two main approaches are used: statistical or physically based model.
In this paper three physically based models for landslides susceptibility analysis were integrated in the Object Modelling System (OMS) and tested in real world applications. Models presented have an increasing degree of complexity. Effects of three different hydrological components connected to the stability model and of model parameters optimization were investigated.
Their integration in OMS allows the use of other components such as GIS tools to manage inputs-output processes, and automatic calibration algorithms to estimate model parameters. Finally, model performances were quantified by using traditional goodness of fit indices such as accuracy, bias score, hit rate, and success index. This research was funded by PON Project No. 01_01503 “Integrated Systems for Hydrogeological Risk Monitoring, Early Warning and Mitigation Along the Main Lifelines”, CUP B31H11000370005, in the framework of the National Operational Program for "Research and Competitiveness" 2007-2013.

***Keywords**:* Landslide modelling; Object Modeling System; Models calibration.

1 INTRODUCTION

Landslide hazard is defined as the probability of occurrence of a potentially damaging phenomenon (landslide) within a given area and in a given period of time” (Varnes et al., 1984). This definition implies the answer to three research questions: where (locations), when (timing) and at which magnitude (size) landslides could happen (Hutchinson, 1995 and references therein). Estimation of landslide susceptibility answers to the first of the previous questions, i.e. where landslides likely occur. Landslide susceptibility is formally defined as the likelihood of a landslide occurring in an area on the basis of local terrain conditions (Brabb, 1984).
Prediction of landslide susceptibility involves different disciplines such as geology, geomorphology, hydrology, and climatology, because landslide occurrence depends on many local concurrent factors. Those can be quasi-static such as slope, geology, and geotechnical soil properties or dynamic such as water table position, soil degree of saturation, root cohesion, and human activities (Rosso et al., 2006, Wu and Sidle, 1995). Many methods for landslide susceptibility mapping were developed and they can be grouped in two main branches: qualitative and quantitative methods (Glade and Crozier, 2005). Qualitative methods as landslide inventories (Bulut et al, 2000) and heuristic approaches (Lee et al., 2002) are based on field campaigns, aerial photograph interpretation and personal knowledge and experience. They are subjective and difficult to be extended in different areas. Quantitative methods include empirical, statistical and deterministic approaches. The empirical methods (Reichenbach et al., 1998, Capparelli and Tiranti, 2010) define empirical thresholds on hydrological variables such as rainfall and soil moisture that trigger the landslide. When thresholds are exceeded landslides are likely triggered.
Statistical methods search functional relationships between instability factor maps (such as geology, soils, slope, curvature, and aspect) and past and present landslide distribution from inventory maps.

They are the most popular and they are based on bivariate (Naranjo et al., 1994) or multivariate (Chung et al. 1995) analysis, discriminant analysis (Guzzetti et al., 1999), artificial neural networks (Conforti et al., 2014 and references therein).
Deterministic models provide a theoretical framework linking hydrology, geomorphology, and geotechnical science with different degree of simplification in order to physically understand landslide location and timing. Infinite slope stability analysis (Duncan and Write, 2005) is usually coupled with steady state (Montgomery and Dietrich, 199, Lu and Godt, 2008) quasi-steady state (Borga et al., 2002) and transient (Iverson, 2000, Baum et al., 2002, Simoni et al., 2008, Capparelli and Versace, 2011) infiltration conditions in order to compute the safety factor FS.
The paper presents a modeling system that contains different type of deterministic models for shallow landslide susceptibility analysis integrated in NewAge-JGrass (Formetta et al., 2014) by using the Object Modeling System (OMS, David et al., 2013) modeling framework. The system contains models, automatic calibration algorithms for model parameters estimation, methods for estimating the goodness of the models prediction. The open source GIS uDig (http://udig.refractions.net/) is used as visualization system. Models can be easily applied, calibrated, compared by using quantitative and qualitative indicators. A case study is presented in order to show all the capability of the system.

2 MODELING SYSTEM

A system for landslide susceptibility analysis is implemented in the context of NewAge-JGrass (Formetta et al., 2014), an open source large-scale hydrological modeling system. It models the whole hydrological cycle: water balance, energy balance, snow melting, etc. It implements automatic calibration algorithms for model parameter optimisation and applications were presented in (Formetta et al., 2011). NewAge-JGrass is a component-based model: each component can be linked and executed at runtime. This is accomplished by OMS (David et al., 2013), a Java based modeling framework that promotes the idea of programming by components. The single scientific building blocks are named OMS components.
The system for landslide susceptibility analysis is presented in the next subsections: the models (subsection 2.1), the system for model verification (subsection 2.2) and the automatic calibration procedure (subsection 2.3). Models are applied in in Calabria (Italy) in order to investigate landslide susceptibility along the Salerno-Reggio Calabria highway in the context of the PON “Integrated Systems for Hydrogeological Risk Monitoring, Early Warning and Mitigation Along the Main Lifelines”.

2.1 Landslide susceptibility models

Landslide susceptibility models since the most famous Shalstab (Montgomery and Dietrich, 1994) couple a slope stability model and a hydrological model in order to estimate susceptible landslide areas. We incorporate in our model the infinite slope equation (Grahm J., 1984) for the factor of safety (ratio of stabilizing to destabilizing forces):

$$FS = \frac{C}{\left[(1-w)\cdot\gamma + w\cdot\gamma_s\right]\cdot H\cdot\sin\alpha\cdot\cos\alpha} + \frac{\left[(1-w)\cdot\gamma + w\cdot\gamma'\right]}{\left[(1-w)\cdot\gamma + w\cdot\gamma_s\right]}\cdot\frac{\tan\varphi'}{\tan\alpha} \qquad (1)$$

where: FS is the factor of safety, C=C’+C_{root} is the sum of C_{root}, the root cohesion [kN/m2], and C’, the effective cohesion [kN/m2], φ' [-] is the internal friction angle, γ the average bulk specific weight of soil [kN/m3], H is the soil depth [m], α [-] is the slope gradient, γ_s the saturated specific weight of soil [kN/m3], $\gamma' = \gamma_s - \gamma_w$ is the submerged specific weight of soil, γ_w is the specific weight of water and w=h/H where h is the water table height above the failure surface [m]. γ, γ_s and γ' are related to the specific gravity of solids Gs [-], average void ratio e [-] and average degree of saturation Sr by equations (2), (3) and (4):

$$\frac{\gamma'}{\gamma_w} = \frac{G_s - 1}{1+e} \qquad (2) \qquad \frac{\gamma}{\gamma_w} = \frac{G_s + e\cdot S_r}{1+e} \qquad (3) \qquad \frac{\gamma_s}{\gamma_w} = \frac{G_s + e}{1+e} \qquad (4)$$

Substituting eq. (2), (3), and (4) into eq. (1) FS can be expressed as:

$$FS = \frac{C \cdot (1+e)}{\left[G_s + e \cdot S_r + w \cdot e \cdot (1-S_r)\right] \cdot \gamma_w \cdot H \cdot \sin\alpha \cdot \cos\alpha} + \frac{\left[G_s + e \cdot S_r - w \cdot (1+e \cdot S_r)\right]}{\left[G_s + e \cdot S_r + w \cdot e \cdot (1-S_r)\right]} \cdot \frac{\tan\varphi'}{\tan\alpha} \quad (5)$$

The first component (M1) is shalstab model (Montgomery and Dietrich, 1994). In this model cohesion, degree of soil saturation and void ratio effect is neglected. Moreover shalstab assumes hydrological steady state and flow occurring in the direction parallel to the slope. Based on those assumptions w is computed as:

$$w = \frac{h}{H} = \min\left(\frac{Q}{T} \cdot \frac{TCA}{b \cdot \sin\alpha}, 1.0\right) \quad (6)$$

where T [L2/T] is the soil transmissivity defined as the product of the soil depth and the saturated hydraulic conductivity. Substituting eq.(6) in (5) the model can be solved for Q/T assuming FS=1:

$$\frac{Q}{T} = \frac{\gamma_s}{\gamma_w} \cdot \left(1 - \frac{\tan\alpha}{\tan\varphi'}\right) \cdot \frac{b \cdot \sin\alpha}{TCA} \quad (7)$$

where b [L] is the length of the contour line. Accordingly, stable and unstable sites are defined using threshold values on log(Q/T).
The second component (M2) implements eq. (5) coupled with eq. (6) (Rosso et al., 2006, Park et al., 2013). Differently from the first component, it considers both soil properties (as degree of soil saturation and void ratio) and the soil cohesion as stabilising factors. The result is a map of safety factors for each pixel of the analysed area. Stable and unstable sites are defined using threshold values on the factor of safety. The threshold value 1 is used in this study.
The last component (M3) relaxes the hypothesis of infinity rainfall duration which is inside the previous models. The model developed by Rosso et al., 2006 considers both the effects of rainfall intensity and duration on the landslide triggering process. In M3 the term w, differently from eq.(6), depends also on rainfall duration and it is obtained by coupling the conservation of mass of soil water with the Darcy's law (Rosso et al., 2006) providing:

$$w = \begin{cases} \frac{Q}{T} \cdot \frac{TCA}{b \cdot \sin\alpha} \cdot \left[1 - \exp\left(\frac{e+1}{e \cdot (1-S_r)} \cdot \frac{t}{T} \cdot \frac{TCA}{b \cdot \sin\alpha} \cdot H\right)\right] & if \ \frac{t}{T} \cdot \frac{TCA}{b \cdot \sin\alpha} \cdot H \le -\frac{e \cdot (1-S_r)}{1+e} \cdot \ln\left(1 - \frac{T \cdot b \cdot \sin\alpha}{TCA \cdot Q}\right) \\ 1 & if \ \frac{t}{T} \cdot \frac{TCA}{b \cdot \sin\alpha} \cdot H > -\frac{e \cdot (1-S_r)}{1+e} \cdot \ln\left(1 - \frac{T \cdot b \cdot \sin\alpha}{TCA \cdot Q}\right) \end{cases} \quad (8)$$

Each component has a user interface where the user specifies input and output. All is embedded in the open source uDig by using the Spatial Toolbox.

2.2 Automatic calibration and model verification procedure

In order to assess the models' performance we developed a package containing the most used indices for assessing the quality of the landslide susceptibility map. These are based on pixel-by-pixel comparison between true mapped landslides (ML), a binary map with "landslide" or "not-landslide" pixels, and predicted landslides (PL), a binary map with "stable" or "unstable" pixels. Therefore, four types of outcomes are possible for each cell. A pixel is a true-positive (tp) if it is mapped as "landslide" in ML and "not stable" in PL. A pixel is a true-negative (tn) if it is mapped as "not-landslide" in ML and "stable" in PL. A pixel is a false-positive (fp) if it is mapped as "not-landslide" in ML and "not-stable" in PL. A pixel is a false- negative (fn) if it is mapped as "landslide" in ML and "stable" in PL. The indices of goodness of fit are implemented in the system. Table. (1) shows their definition, range, and optimal values.
Automatic calibration models implemented in OMS and in NewAge-JGrass can be used in order to tune model parameters for reproducing the actual landslide. This is possible because each model is an OMS component and can be linked to the calibration algorithms as it is, without rewriting or

modifying their code. Two calibration algorithms are embedded in OMS core: Luca (Hay et al., 2006), a step-wise algorithm based on shuffle complex evolution (Duan et al., 1992), and Particle swarm optimisation (PSO), a genetic model presented in (Kennedy and Eberhart, 1995). Independently of the calibration algorithm used, model output obtained with different parameters values are compared with actual landslide map by using one of the metrics presented in the previous subsection (Equitable Success Index).

Index	Definition	Range	Optimal Value
Accuracy	$ACC=\frac{tp+tn}{tp+fn+fp+tn}$	[0 ;1]	1
Critical success index	$CSI=\frac{tp}{tp+fp+fn}$	[0 ;1]	1
Equitable success index	$ESI=\frac{tp-R}{tp+fp+fn-R}$ $R=\frac{(tp+fn)\cdot(tp+fp)}{tp+fn+fp+tn}$	[-1/3;1]	1
True Positive Rate	$TPR=\frac{tp}{tp+fn}$	[0;1]	1
False Positive Rate	$FPR=\frac{fp}{fp+tn}$	[0;1]	0
Distance to perfect classification	$D2PC=\sqrt{(1-TPR)^2+FPR^2}$	[0 ;1]	0
True Skill Statistic	$TSS=\frac{(tp\cdot tn)-(fp\cdot fn)}{(tp+fn)\cdot(fp+tn)}$	[-1;1]	1

Table 1: Indices of goodness of fit for comparison between actual and predicted landslide.

3 MODEL APPLICATION

The system presented in the paper is applied for the highway Salerno-Reggio Calabria in Calabria region (Italy), between Cosenza and Altilia, Fig. (1). A map of shallow landslides was derived from a field and photo analysis and landslides are split into two groups one for calibration and one for verification. The resulting maps are presented in Fig. (2).

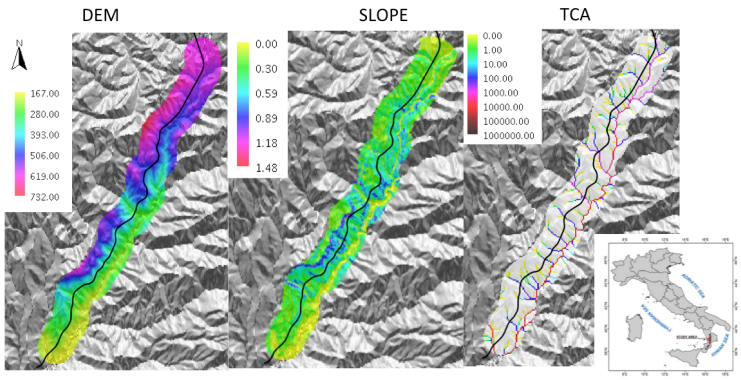

Figure 1: Test site. Digital elevation model (DEM) [m], slope [-] expressed as tangent of the angle and total contributing area (TCA) expressed as number of draining cells.

The three models were applied and models' parameters were optimized using PSO in order to fit landslides of the calibration group. Finally models' performance is evaluated for landslides of the verification group. The application aims to show the effects of the different hydrological components implemented in each model and contributes of cohesion and soil properties to the hillslope stability. Optimal parameters' sets and model performance results are presented in tables 2 and 3 respectively.

Model Parameters	M1	M2	M3
Soil Depth [m]	1.95	1.5	1.3
Transmissivity [m2/d]	10.0	43	84
Soil Specific weight [kN/m3]	19	21	20
Friction Angle [°]	29	31	30
Rainfall [mm/d]	198	70	153
Soil Cohesion [kPa]	-	6	4
Degree Of Saturation [-]	-	25	58
Rainfall Duration [d]	-	-	1.2

Table 2: Optimised models' parameters values

	Calibration			Verification		
Index	M1	M2	M3	M1	M2	M3
Accuracy	0.66	0.68	0.72	0.61	0.63	0.68
True Positive Rate	0.65	0.68	0.71	0.65	0.66	0.68
False Positive Rate	0.36	0.33	0.31	0.37	0.34	0.33

Table 3: Goodness of fit indices for calibration and verification period

Results confirm that moving from models M1 to M3 and taking into account soil properties and rainfall duration increase the reliability of landslides susceptibility map. This is confirmed both in calibration and in verification period by the goodness of fit indices reported in table 3. Model M1 overestimate the unstable pixels: it shows the higher value of false positive rate and the lower value of true positive rate in both calibration and verification period. Model M2, which take into account soil properties such as degree of saturation, soil porosity and cohesion, reduces the false positive rate from 0.36 to 0.33 and increase the true positive rate from 0.65 to 0.68. Finally the best results are reached with the model M3 that considers a rainfall of finite duration. The results are qualitatively presented in Fig. (2). For each model (M1, M2 and M3) it shows two maps: the maps of true positive and true negative (in blue) and the maps of false positive and false negative (in red) on the left-hand side (named T1 in the text); a perfect model should have just blue pixel. The second map superimposes the predicted unstable (red) and stable (yellow) pixels and the shape file of the actual landslides, on the right-hand side (named T2 in the text). Moving from M1 to M3, T1 reduces the number of false positive and false negative (red pixels) and T2 became more accurate in detection of actual unstable pixels.

4 CONCLUSIONS

A system for landslides susceptibility maps is proposed obtaining possibility to apply models with different degree of complexity. The system is part of NewAge-JGrass, built with OMS framework, and for this reason is able to use: i) components for evaluating performance of predictions; ii) model parameters calibration algorithms for estimating optimal parameter set and iii) the GIS uDig for input maps preparation and output visualisation. Models can be executed by OMS console or a toolbox embedded in the GIS uDig.

A case study is presented in order to test all the system capabilities. The test site is in Calabria (Italy) along the A3-highway between Cosenza and Rogliano. Model parameters were optimised in order to fit maps of actual shallow landslides in the monitored site. Comparisons between three different models were performed and the best model for the case study resulted M3. It reached the best performance in terms of true positive rate and a decrement of false positive rate compared to M1 and M2, both in calibration and in validation period.

ACKNOWLEDGMENTS

This research was funded by PON Project No. 01_01503 "Integrated Systems for Hydrogeological Risk Monitoring, Early Warning and Mitigation Along the Main Lifelines", CUP B31H11000370005, in the framework of the National Operational Program for "Research and Competitiveness" 2007-2013

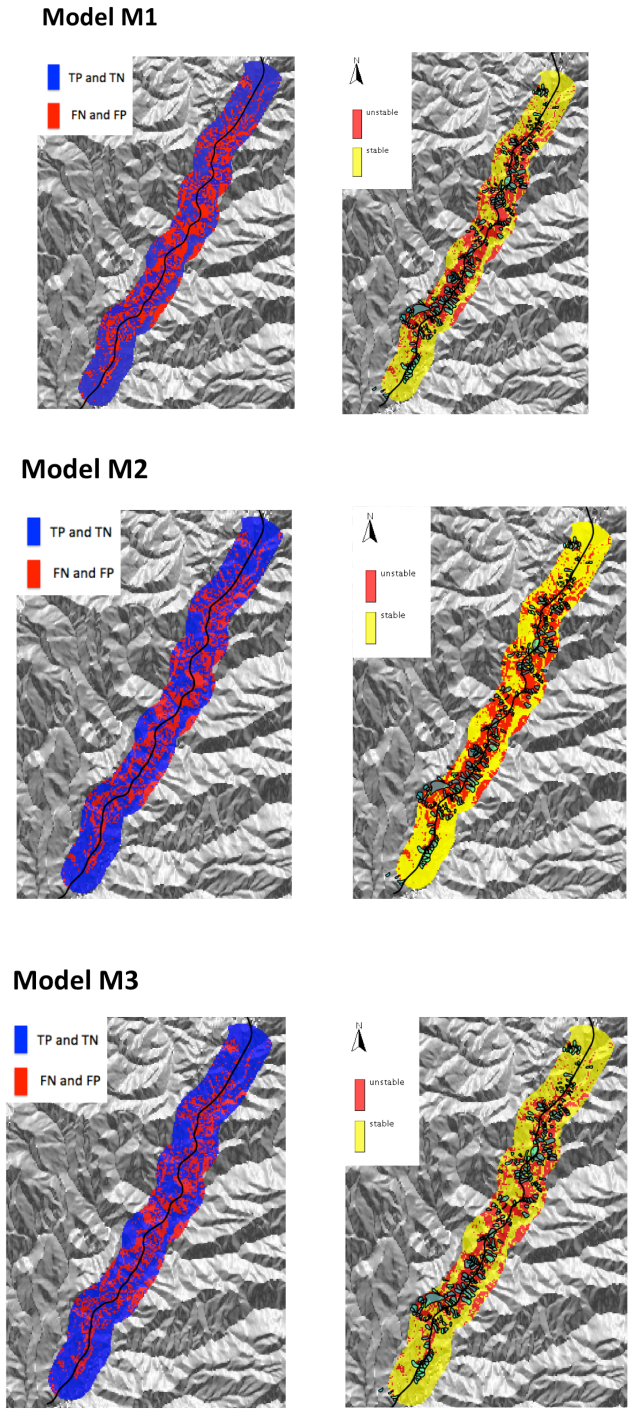

Figure 2: Maps of the true positive and true negative (in blue) and of false positive and false negative (in red) on the left and maps of actual landslides and stable (in red) and unstable (in yellow) predicted pixels on the right.

REFERENCES

Baum, R., Savage, W., and Godt, J, (2002) TRIGRS A fortran program for transient rainfall infiltration and grid-based regional slope-stability analysis, US Geological Survey Open Report, 424, 61

Borga, M., Dalla Fontana, G., & Cazorzi, F. (2002). Analysis of topographic and climatic control on rainfall-triggered shallow landsliding using a quasi-dynamic wetness index. Journal of Hydrology, 268(1), 56-71.

Brabb, E.E., (1984). Innovative approaches to landslide hazard and risk mapping, Proceedings of the 4th International Symposium on Landslides, 16–21 September, Toronto, Ontario, Canada (Canadian Geotechnical Society, Toronto, Ontario, Canada), 1:307–324

Bulut, F., Boynukalin, S., Tarhan, S. and Ataoglu, E. (2000) Reliability of landslide isopleth maps. Bulletin of Engineering Geology and the Environment, 58:2 95-98.

Capparelli, Giovanna, and Davide Tiranti, (2010) "Application of the MoniFLaIR early warning system for rainfall-induced landslides in Piedmont region (Italy)." Landslides 7.4: 401-410.

Capparelli, G., & Versace, P. (2011). FLaIR and SUSHI: two mathematical models for early warning of landslides induced by rainfall. Landslides, 8(1), 67-79.

Chung C-JF, Fabbri AG and van Westen CJ (1995) Multivariate regression analysis for landslide hazard zonation. Carrara A and Guzzetti F (Eds.) Geographical Information Systems in assessing natural hazards. Dordrecht, Kluwer Academic Publishers. 5:107-34

Conforti, M., Pascale, S., Robustelli, G., & Sdao, F. (2014). Evaluation of prediction capability of the artificial neural networks for mapping landslide susceptibility in the Turbolo River catchment (northern Calabria, Italy). Catena, 113, 236-250.

David, O., Ascough II, J. C., Lloyd, W., Green, T. R., Rojas, K. W., Leavesley, G. H., & Ahuja, L. R. (2013). A software engineering perspective on environmental modeling framework design: The Object Modeling System. *Environmental Modelling & Software*, *39*, 201-213.

Duan, Q., Sorooshian S., and Gupta V(1992): Effective and efficient global optimization for conceptual rainfall-runoff models. Water Resources Research 28.4 (1992): 1015-1031.

Duncan, J. M., and S. G. Wright (2005), Soil Strength and Slope Stability, 297 pp., John Wiley.

Formetta, G., Mantilla, R., Franceschi, S., Antonello, A., & Rigon, R. (2011). The JGrass-NewAge system for forecasting and managing the hydrological budgets at the basin scale: models of flow generation and propagation/routing. *Geoscientific Model Development*, *4*(4), 943-955.

Formetta, G., Antonello, A., Franceschi, S., David, O., & Rigon, R. (2014). Hydrological modelling with components: A GIS-based open-source framework. *Environmental Modelling & Software*, *55*, 190-200.

Glade, T., & Crozier, M. J. (2005). A review of scale dependency in landslide hazard and risk analysis. Landslide hazard and risk, 75-138.

Grahm J (1984) Methods of slope stability analysis. In: Brunsden D, Prior DB (eds) Slope instability. Wiley, New York, pp 171–215

Hutchinson, J. N. (1995): Keynote paper: Landslide hazard assessment. In: Bell (ed.), Landslides, Balkema, Rotterdam, 1805–1841,

Hay, L.E., G.H. Leavesley, M.P. Clark, S.L. Markstrom, R.J. Viger, and M. Umemoto (2006). Step-Wise, Multiple-Objective Calibration of a Hydrologic Model for a Snowmelt-Dominated Basin. Journal of the American Water Resources Association 42:877-890, 2006

Kennedy, J., and Eberhart R.(1995): Particle swarm optimization. Neural Networks, 1995. Proceedings., IEEE International Conference on. Vol. 4. IEEE, 1995.

Iverson RM. 2000. Landslide triggering by rain infiltration. Water Resources Research 36(7): 1897–1910

Lee, S., Chwae, U. and Min, K. (2002) Landslide susceptibility mapping by correlation between topography and geological structure: the Janghung area, Korea. Geomorphology, 46:3-4 149-162

Lu, N., & Godt, J. (2008). Infinite slope stability under steady unsaturated seepage conditions. Water resources research, 44(11).

Montgomery, D. R., & Dietrich, W. E. (1994). A physically based model for the topographic control on shallow landsliding. *Water resources research*, *30*(4), 1153-1171.

Naranjo, J.L., van Westen, C.J. and Soeters, R. (1994) Evaluating the use of training areas in bivariate statistical landslide hazard analysis: a case study in Colombia. ITC Journal, 3:292-300.

Park, H. J., Lee, J. H., & Woo, I. (2013). Assessment of rainfall-induced shallow landslide susceptibility using a GIS-based probabilistic approach. *Engineering Geology*, *161*, 1-15.

Reichenbach, P., Cardinali, M., De Vita, P., & Guzzetti, F. (1998). Regional hydrological thresholds for landslides and floods in the Tiber River Basin (central Italy). Environmental Geology, 35(2-3), 146-159.

Rosso, R., Rulli, M. C., & Vannucchi, G. (2006). A physically based model for the hydrologic control on shallow landsliding. *Water Resources Research*, *42*(6).

Simoni, S., Zanotti, F., Bertoldi, G., and Rigon, R. (2008): Modeling the probability of occurrence of shallow landslides and channelized debris flows using GEOtop-FS, Hydrol. Process., 22, 532{545,

Varnes D.J. (1984), and IAEG Commission on Landslides and other Mass Movements, Landslide hazard zonation: a review of principles and practice. UNESCO Press, Paris, 63 p.

Wu,W., Sidle, R.C., (1995). A distributed slope stability model for steep forested basins. Water Resource